

## Thermal buckling behaviour of shear deformable functionally graded single/doubly curved shell panel with TD and TID properties

Vishesh R. Kar<sup>1a</sup>, Subrata K. Panda<sup>\*2</sup> and Trupti R. Mahapatra<sup>3b</sup>

<sup>1</sup>Department of Design and Automation, School of Mechanical Engineering,  
VIT University Vellore: 632014, India

<sup>2</sup>Department of Mechanical Engineering, National Institute of Technology, Rourkela: 769008, India

<sup>3</sup>School of Mechanical Engineering, KIIT University, Bhubaneswar: 751024, India

(Received July 20, 2016, Revised November 28, 2016, Accepted November 30, 2016)

**Abstract.** In this article, the buckling responses of functionally graded curved (spherical, cylindrical, hyperbolic and elliptical) shell panels under elevated temperature load are investigated numerically using finite element steps. The effective material properties of the functionally graded shell panel are evaluated using Voigt's micromechanical model through the power-law distribution with and without temperature dependent properties. The mathematical model is developed using the higher-order shear deformation theory in conjunction with Green-Lagrange type nonlinear strain to consider large geometrical distortion under thermal load. The efficacy of the proposed model has been checked and the effects of various geometrical and material parameters on the buckling load are analysed in details.

**Keywords:** FGM; thermal buckling; single/doubly curved panel; HSDT; ANSYS

---

### 1. Introduction

Functionally graded material (FGM) is microscopically heterogeneous which is achieved through the gradation of two or more materials from one surface to another. The typical FGM constituents are metal/alloy and ceramic materials. The advantages of these materials, such as high fracture toughness in metal and high heat-resistant in ceramic, make FGM be the one of the promising material under severe environmental conditions. The structures made up of FGM are more significant in aerospace, defence, energy, etc. for thermal barrier applications. The FGM structures exposed to the high-temperature environment cause the instability in geometry. Therefore, it has become the necessity that the buckling behaviour of FGM structures under the thermal environment has to be analysed. In this regard, many studies on the stability of FGM structures like flat/curved panels are presented in past.

Some of the contributions to the closed-form solutions of the buckling load parameter of the

---

\*Corresponding author, Assistant Professor, E-mail: [call2subrat@gmail.com](mailto:call2subrat@gmail.com)

<sup>a</sup>Assistant Professor, E-mail: [visheshkar@gmail.com](mailto:visheshkar@gmail.com)

<sup>b</sup>Assistant Professor, E-mail: [trmahapatrafme@gmail.com](mailto:trmahapatrafme@gmail.com)

functionally graded (FG) flat panels are presented by taking the geometrical imperfections under various mechanical and thermal loading conditions (Javaheri and Eslami 2002a, b, c, Shariat *et al.* 2005, Shariat and Eslami 2005, 2006, 2007, Lanhe 2004). The mathematical models in the above-discussed studies are developed using various mid-plane kinematics such as the classical plate theory (CPT), the first-order shear deformation theory (FSDT) and the higher-order shear deformation theory (HSDT) and von-Karman type geometrical distortion due to thermal load. Na and Kim (2004) examined the thermal buckling behaviour of the FG plate using finite element method (FEM) through a 3D eight noded solid element. Shahsiah and Eslami (2003) studied the buckling behaviour of simply-supported FG cylindrical shell panel using the FSDT and Sander's nonlinear kinematics. Mahi *et al.* (2015) proposed a new hyperbolic shear deformation theory to investigate the static and the free vibration behaviour of isotropic/layered/sandwich/FG composite plates. Ganapathi and his co-workers (Ganapathi and Prakash 2006 and Ganapathi *et al.* 2006) investigated the buckling behaviour of simply-supported FG skew plate under thermal and mechanical load using the FSDT mid-plane kinematics and finite element (FE) approach. Zhao *et al.* (2009) reported the buckling load parameter of the FG flat panel using the element-free kp-Ritz method in the framework of the FSDT kinematics. Owing to the simplicity in formulation and effective computational ability various HSDTs are more popularly applied to FG structures in comparison to other existing layer wise theories in recent past (Bouderba *et al.* 2013, Tounsi *et al.* 2013, Heballi *et al.* 2014, Meziane *et al.* 2014, Bousahla *et al.* 2014, Belabed *et al.* 2014, Bourada *et al.* 2015, Yahia *et al.* 2015, Hamidi *et al.* 2015, Daouadji *et al.* 2016, Bennoun *et al.* 2016, Bourada *et al.* 2016, Bellifa *et al.* 2016, Bounouara *et al.* 2016). In addition to these, we also note that many researchers have put forward numerous efficient refined HSDTs to analyse the buckling and vibration responses of FG plates (Bouiadjra *et al.* 2012, Thai and Choi 2012, Zidi *et al.* 2014, Tounsi *et al.* 2016, Houari *et al.* 2016). Ghannadpour *et al.* (2012) employed finite strip method to analyse the buckling behaviour of FG plate under thermal environment using Green's strain. Abdelhak *et al.* (2015) analysed thermal buckling behaviour of FGM plate using an  $n^{\text{th}}$  order four variable theory. Pradyumna and Bandyopadhyay (2010) reported the FEM solutions of the free vibration and the buckling responses of the FG curved shell panel under temperature field using the HSDT mid-plane kinematics. Topal and Uzman (2009) reported thermal buckling optimisation of symmetrically laminated cylindrical shell panel using the FSDT kinematics under uniform thermal load. Bourada *et al.* (2011) reported a new four parameter based hyperbolic shear deformable theory for the analysis of the thermal buckling behaviour of the FGM structure. In addition, some of the research related to the buckling and postbuckling strength of the laminated structures under the elevated thermal environment including the effect of smart layers are reported using the HSDT kinematics and Green-Lagrange nonlinearity by Panda and his co-authors. (2009, 2010a, 2010b, 2011, 2013, 2013a, 2013b, 2013c, 2015, 2015a, 2015b, 2015)

From the above review, it is observed that most of the studies on the buckling behaviour are presented for the FG flat panel with von-Karman type nonlinear kinematics instead of the curved panel and Green-Lagrange type nonlinearity. In this present article, authors' aim to analyse the buckling behaviour of FG shell panels of different shell geometries (spherical, cylindrical, hyperbolic and elliptical panels) under two types of temperature field (uniform and linear). In this study, the FG shell panel properties are evaluated using Voigt's rule of mixture in conjunction with the power law of distribution by taking temperature-dependent (TD) and temperature-independent (TID) properties. The mathematical model is developed based on the HSDT and Green-Lagrange type nonlinear strain kinematics for the geometrical distortion under temperature load. In addition, all the nonlinear higher terms are included in the geometry matrix to count the large geometrical

distortions under different thermal environment and predict the exact buckling strength of the FG shell panels of different geometries. The buckling load parameter of the present FG shell panel is computed numerically with the help of presently developed FE model in conjunction with the homemade computer code developed in MATLAB environment. The efficacy of the present numerical results has been checked by comparing the responses with those available published results as well as the simulation values. The simulation results are computed using the commercial FE tool (ANSYS) with the help of ANSYS parametric design language (APDL) code. Finally, the importance of the proposed higher-order model with Green-Lagrange type of nonlinear strain kinematics for the evaluation of the geometry matrix has been highlighted in details by solving numerous examples.

## 2. Theoretical development and finite element formulation

In this present study, a general mathematical model is developed for the single/doubly curved shell panel with principal radii of curvatures say,  $R_x$  (with respect to the  $x$ - direction),  $R_y$  (with respect to the  $y$ - direction) and  $R_{xy}$  (twist radius/ in-plane radius as infinite). The shell geometries such as spherical, cylindrical, hyperbolic and elliptical panels are defined from the general doubly curved shell panel as  $R_x=R_y=R$ ;  $R_x=R, R_y=\infty$ ;  $R_x=R, R_y=-R$  and  $R_x=R, R_y=2R$ , respectively as in Fig. 1. Here,  $R$  is any constant value for the radius of curvature. The total thickness of the shell panel is assumed to be  $h$ . The planar form of the curved shell panel on the  $xy$  plane is considered in the rectangular form of length ' $a$ ' and width ' $b$ '.

### 2.1 Kinematic model

In this study, the displacement field of the FG curved shell panel is derived based on the HSDT kinematics in the mid-plane of the shell panel (at  $z=0$ ). The global displacements ( $u, v, w$ ) are

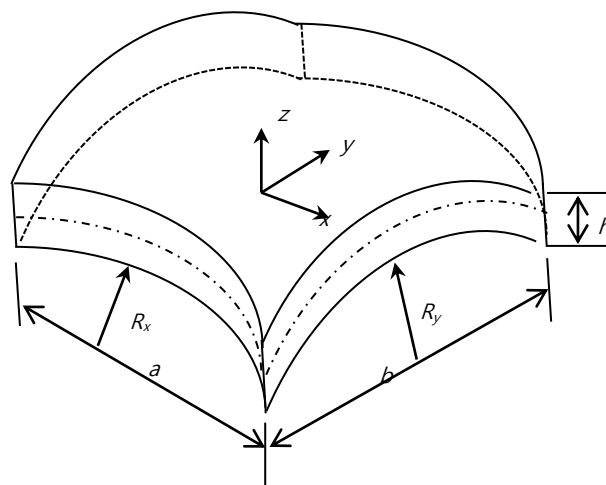


Fig. 1 A doubly curved FG shell panel

defined in the following polynomial form of nine unknown parameters as in Kar and Panda (2015)

$$u = u_0 + z\theta_x + z^2u_0^* + z^3\theta_x^*; \quad v = v_0 + z\theta_y + z^2v_0^* + z^3\theta_y^*; \quad w = w_0 \quad (1)$$

where,  $(u_0, v_0, w_0)$  denote the mid-plane displacements along  $(x, y, z)$  coordinates, respectively.  $\theta_y$  and  $\theta_x$  are the shear rotations about the  $x$ - and  $y$ -axis, respectively and  $(u_0^*, v_0^*, \theta_x^*, \theta_y^*)$  are the higher-order terms defined in the mid-plane of the curved panel. These nine unknowns can be defined in the mid-plane, i.e., at  $z=0$  as  $u_0=u(x,y,t)$ ,  $v_0=v(x,y,t)$ ,  $w_0=w(x,y,t)$ ,  $\theta_x = \frac{\partial u}{\partial z}$ ,  $\theta_y = \frac{\partial v}{\partial z}$ ,

$$u_0^* = \frac{1}{2} \left( \frac{\partial^2 u}{\partial z^2} \right), \quad v_0^* = \frac{1}{2} \left( \frac{\partial^2 v}{\partial z^2} \right), \quad \theta_x^* = \frac{1}{6} \left( \frac{\partial^3 u}{\partial z^3} \right) \quad \text{and} \quad \theta_y^* = \frac{1}{6} \left( \frac{\partial^3 v}{\partial z^3} \right).$$

## 2.2 Strain-displacement relations

The strain tensor ( $\varepsilon$ ) at any point for the FG doubly curved panel is given by

$$\varepsilon = \begin{Bmatrix} \varepsilon_{xx} \\ \varepsilon_{yy} \\ \gamma_{xy} \\ \gamma_{xz} \\ \gamma_{yz} \end{Bmatrix} = \begin{Bmatrix} u_{,x} \\ v_{,y} \\ u_{,y} + v_{,x} \\ u_{,z} + w_{,x} \\ v_{,z} + w_{,y} \end{Bmatrix} = \left\{ \left( \frac{\partial u}{\partial x} + \frac{w}{R_x} \right) \left( \frac{\partial v}{\partial y} + \frac{w}{R_y} \right) \left( \frac{\partial u}{\partial y} + \frac{\partial v}{\partial x} + \frac{2w}{R_{xy}} \right) \left( \frac{\partial u}{\partial z} + \frac{\partial w}{\partial x} - \frac{u}{R_x} \right) \left( \frac{\partial v}{\partial z} + \frac{\partial w}{\partial y} - \frac{v}{R_y} \right) \right\}^T \quad (2)$$

Eq. (2) can also be rewritten in the mid-plane form as

$$\begin{Bmatrix} \varepsilon_{xx} \\ \varepsilon_{yy} \\ \gamma_{xy} \\ \gamma_{xz} \\ \gamma_{yz} \end{Bmatrix} = \begin{Bmatrix} \varepsilon_x^0 \\ \varepsilon_y^0 \\ \varepsilon_{xy}^0 \\ \varepsilon_{xz}^0 \\ \varepsilon_{yz}^0 \end{Bmatrix} + z \begin{Bmatrix} k_x^1 \\ k_y^1 \\ k_{xy}^1 \\ k_{xz}^1 \\ k_{yz}^1 \end{Bmatrix} + z^2 \begin{Bmatrix} k_x^2 \\ k_y^2 \\ k_{xy}^2 \\ k_{xz}^2 \\ k_{yz}^2 \end{Bmatrix} + z^3 \begin{Bmatrix} k_x^3 \\ k_y^3 \\ k_{xy}^3 \\ k_{xz}^3 \\ k_{yz}^3 \end{Bmatrix} = [T] \{ \bar{\varepsilon} \} \quad (3)$$

where,  $[T]$  is the thickness coordinate matrix  $(1, z, z^2, z^3)$  associated with the mid-plane strain terms  $\{ \bar{\varepsilon} \}$ . The individual strain vectors are given by as follows

$$\begin{Bmatrix} \varepsilon_x^0 \\ \varepsilon_y^0 \\ \varepsilon_{xy}^0 \\ \varepsilon_{xz}^0 \\ \varepsilon_{yz}^0 \end{Bmatrix} = \begin{Bmatrix} \frac{\partial u_0}{\partial x} + \frac{w_0}{R_x} \\ \frac{\partial v_0}{\partial y} + \frac{w_0}{R_y} \\ \frac{\partial u_0}{\partial y} + \frac{\partial v_0}{\partial x} + \frac{2w_0}{R_{xy}} \\ \frac{\partial w_0}{\partial x} - \frac{u_0}{R_x} + \theta_x \\ \frac{\partial w_0}{\partial y} - \frac{v_0}{R_y} + \theta_y \end{Bmatrix}, \quad \begin{Bmatrix} k_x^1 \\ k_y^1 \\ k_{xy}^1 \\ k_{xz}^1 \\ k_{yz}^1 \end{Bmatrix} = \begin{Bmatrix} \frac{\partial \theta_x}{\partial x} \\ \frac{\partial \theta_y}{\partial y} \\ \frac{\partial \theta_x}{\partial y} + \frac{\partial \theta_y}{\partial x} \\ 2u_0^* - \frac{\theta_x}{R_x} \\ 2v_0^* - \frac{\theta_y}{R_y} \end{Bmatrix}, \quad \text{and} \quad \begin{Bmatrix} k_x^3 \\ k_y^3 \\ k_{xy}^3 \\ k_{xz}^3 \\ k_{yz}^3 \end{Bmatrix} = \begin{Bmatrix} \frac{\partial \theta_x^*}{\partial x} \\ \frac{\partial \theta_y^*}{\partial y} \\ \frac{\partial \theta_x^*}{\partial y} + \frac{\partial \theta_y^*}{\partial x} \\ -\frac{\theta_x^*}{R_x} \\ -\frac{\theta_y^*}{R_y} \end{Bmatrix} \quad (4)$$

### 2.3 Effective material properties of FGM

As discussed earlier, the present FGM shell panel properties are varying gradually from the bottom surface ( $z=-h/2$ ) to the top surface ( $z=+h/2$ ). The ceramic and the metals are the two constituents of the present FGM shell at the top and the bottom of the panel, respectively. The properties of the FGM constituents are assumed to be temperature-dependent (Reddy and Chin 1998) and expressed as

$$\xi_{c,m}(T) = \xi_0(\xi_{-1}T^{-1} + 1 + \xi_1T + \xi_2T^2 + \xi_3T^3) \quad (5)$$

where, subscript 'c' and 'm' represent the ceramic and the metal constituents, respectively.  $\xi_0$ ,  $\xi_{-1}$ ,  $\xi_1$ ,  $\xi_2$  and  $\xi_3$  are the coefficients of temperature ( $T$ ).

The volume fraction of FGM constituents ( $\mathcal{G}_c$  and  $\mathcal{G}_m$ ) are evaluated by incorporating the power-law distribution across the thickness direction and expressed as Shen (2009)

$$\mathcal{G}_c(z) = \left(\frac{z}{h} + \frac{1}{2}\right)^n \quad \text{and} \quad \mathcal{G}_m(z) = 1 - \mathcal{G}_c(z) \quad (6)$$

where,  $n$  represents the power-law index that varies from  $n=0$  (complete ceramic phase) to  $n=\infty$  (full metal phase).

Finally, the material properties of the FGM ( $\zeta$ ) such as Young's modulus ( $E$ ), Poisson's ratio ( $\nu$ ) and coefficient of thermal expansion ( $\alpha$ ) are computed using Voigt's micromechanical model as in (Gibshon *et al.* 1995)

$$\zeta(T, z) = (\zeta_c(T) - \zeta_m(T))\mathcal{G}_c(z) + \zeta_m(T) \quad (7)$$

In this study, two different types of temperature field namely, uniform and linear temperature distributions across the thickness direction of the FG curved panel are considered. The bottom surface temperature ( $T_m$ ) of the FG panel (also referred as reference temperature) is assumed to be at ambient temperature, i.e., 300K. The FG panel is exposed to the elevated temperature ( $T$ ) either uniformly or linearly distributed in the thickness coordinate. The temperature function of the FG panel is expressed in the following form for uniform temperature load

$$T = T_m + \Delta T \quad \text{or} \quad T = T_c \quad (8)$$

where,  $\Delta T$  is the temperature difference between the final and the reference temperature, i.e.,  $\Delta T = T_c - T_m$ .

In the similar fashion, the temperature profile for linear thermal load across the thickness direction is expressed as in the following equation

$$T(z) = T_m + (T_c - T_m) \left(\frac{z}{h} + \frac{1}{2}\right) \quad (9)$$

### 2.4 Constitutive relations

The stress tensor at any point within the FG single/doubly curved panel is given by

$$\sigma = \begin{Bmatrix} \sigma_{xx} \\ \sigma_{yy} \\ \tau_{xy} \\ \tau_{xz} \\ \tau_{yz} \end{Bmatrix} = \begin{bmatrix} Q_{11} & Q_{12} & 0 & 0 & 0 \\ Q_{21} & Q_{22} & 0 & 0 & 0 \\ 0 & 0 & Q_{33} & 0 & 0 \\ 0 & 0 & 0 & Q_{44} & 0 \\ 0 & 0 & 0 & 0 & Q_{55} \end{bmatrix} \begin{Bmatrix} \varepsilon_{xx} \\ \varepsilon_{yy} \\ \gamma_{xy} \\ \gamma_{xz} \\ \gamma_{yz} \end{Bmatrix} - \begin{bmatrix} 1 \\ 1 \\ 0 \\ 0 \\ 0 \end{bmatrix} \alpha \Delta T \quad (10)$$

where,  $Q_{11}=Q_{22}=E/(1-\nu^2)$ ,  $Q_{12}=Q_{21}=E*\nu/(1-\nu^2)$ ,  $Q_{33}=Q_{44}=Q_{55}=E/2*(1+\nu)$ .

Now, the Eq. (10) is rewritten as

$$\{\sigma\} = [Q]\{\varepsilon\} - [Q]\{\varepsilon_{th}\} \quad (11)$$

where,  $[Q]$  is the reduced stiffness matrix and  $\{\varepsilon_{th}\}=[11000]^T \alpha \Delta T$  is the thermal strain tensor.

The total strain energy of the FG curved panel is given by

$$\begin{aligned} U_\varepsilon &= \frac{1}{2} \iint \left[ \int_{-h/2}^{+h/2} \{\varepsilon\}^T \{\sigma\} dz \right] dx dy = \frac{1}{2} \iint \left( \int_{-h/2}^{+h/2} \{\bar{\varepsilon}\}^T [T]^T [Q] [T] \{\bar{\varepsilon}\} dz \right) dx dy \\ &= \frac{1}{2} \iint \left( \{\delta\}^T [B]^T [D] [B] \{\delta\} \right) dx dy \end{aligned} \quad (12)$$

where,  $[D] = \int_{-h/2}^{+h/2} [T]^T [Q] [T] dz$ .

The FG curved panel is subjected to the different thermal load and the total external work done ( $W_T$ ) due to the in-plane thermal force resultant  $\{N_T\}$  can be expressed as in Cook *et al.* (2009)

$$W_T = \int_v \left[ \frac{1}{2} \left\{ (u_{,x})^2 + (v_{,x})^2 + (w_{,x})^2 \right\} N_{Tx} + \frac{1}{2} \left\{ (u_{,y})^2 + (v_{,y})^2 + (w_{,y})^2 \right\} N_{Ty} + \left\{ u_{,x} u_{,y} + v_{,x} v_{,y} + w_{,x} w_{,y} \right\} N_{Txy} \right] dv \quad (13)$$

where,  $\{N_{Tx} \quad N_{Ty} \quad N_{Txy}\}^T = (Q_{11} + Q_{12}) \{1 \quad 1 \quad 0\}^T \alpha \Delta T$  is the thermal force resultant.

Now

$$W_T = \frac{1}{2} \iint \left[ \{\bar{\varepsilon}_G\}^T [D_G] \{\bar{\varepsilon}_G\} \right] dx dy \quad (14)$$

where,  $\{\bar{\varepsilon}_G\}$  and  $[D_G]$  are the in-plane strain vector and the material property matrix, respectively.

## 2.5 Finite element formulation

In this study, the developed higher-order model of the FG curved shell panel is discretised using suitable FE steps. For the discretisation purpose, a nine-noded isoparametric quadrilateral Lagrangian element with eighty-one degrees of freedom per node is employed. The mid-plane displacement field variables can be expressed in the nodal displacement field and their respective shape function as follows

$$\{\delta_0\} = \sum_{i=1}^9 N_i \{\delta_{0_i}\} \tag{15}$$

where,  $N_i$  is the interpolating function of each node and the nodal displacement vector for any  $i^{th}$  node is represented as  $\{\delta_{0_i}\} = [u_{0_i} \ v_{0_i} \ w_{0_i} \ \theta_{x_i} \ \theta_{y_i} \ u_{0_i}^* \ v_{0_i}^* \ \theta_{x_i}^* \ \theta_{y_i}^*]^T$ . The details of the shape function can be seen in Cook *et al.* (2009).

The total mid-plane and geometry strain vectors of the FG curved panel can be expressed as follows

$$\{\bar{\epsilon}\} = [B]\{\delta_0\} \quad \text{and} \quad \{\bar{\epsilon}_G\} = [B_G]\{\delta_0\} \tag{16}$$

where,  $[B]$  and  $[B_G]$  are the product form of the differential operator matrix and the corresponding shape functions, respectively.

### 2.6 System governing equation

The governing equation for the FG curved panel under the thermal environment is derived using variational principle as

$$\delta \Pi = \delta(U_\epsilon - W_T) = 0 \tag{17}$$

Now, by substituting Eqs. (12) to (16) into Eq. (17), the final form of the governing equation of the FG curved panel is conceded to the following form

$$([K] + \lambda_{cr}[K_G])\{\delta\} = 0 \tag{18}$$

where,  $[K] = [B]^T [D] [B]$  and  $[K_G] = [B_G]^T [D_G] [B_G]$  are the system stiffness matrix and the geometrical stiffness matrix, respectively and  $\lambda_{cr}$  is the critical buckling temperature load.

## 3. Results and discussions

In this section, the critical buckling temperature load parameter of the FG curved panel is computed under uniform and linear temperature field through a homemade computer code developed in MATLAB environment based on the proposed HSDT finite element model. In this

Table 1 Material property of the FGM constituents (Reddy 1998)

Material	Properties	TD properties					TID Properties at 300 K
		$\zeta_0$	$\zeta_{-1}$	$\zeta_1$	$\zeta_2$	$\zeta_3$	
SUS304	$E$ (Pa)	$2.0104 \times 10^{11}$	0	$3.079 \times 10^{-4}$	$-6.534 \times 10^{-7}$	0	$2.08 \times 10^{11}$
	$\nu$	0.3262	0	$-2.0 \times 10^{-4}$	$3.8 \times 10^{-7}$	0	0.318
	$\alpha$ (K <sup>-1</sup> )	$1.233 \times 10^{-5}$	0	$8.086 \times 10^{-4}$	0	0	$1.53 \times 10^{-5}$
Si <sub>3</sub> N <sub>4</sub>	$E$	$3.4843 \times 10^{11}$	0	$-3.07 \times 10^{-4}$	$2.16 \times 10^{-7}$	$-8.946 \times 10^{-11}$	$3.22 \times 10^{11}$
	$\nu$	0.24	0	0	0	0	0.24
	$\alpha$	$5.8723 \times 10^{-6}$	0	$9.095 \times 10^{-4}$	0	0	$7.47 \times 10^{-6}$

Table 2 Different types of support conditions

CCCC	$u_0 = v_0 = w_0 = \theta_x = \theta_y = u_0^* = v_0^* = \theta_x^* = \theta_y^* =$ at $x=0, a$ and $y=0, b$
SSSS	$v_0 = w_0 = \theta_y = v_0^* = \theta_y^* =$ at $x=0, a$ ; $u_0 = w_0 = \theta_x = u_0^* = \theta_x^* =$ at $y=0, b$
SCSC	$v_0 = w_0 = \theta_y = v_0^* = \theta_y^* =$ at $x=0, a$ ; $u_0 = v_0 = w_0 = \theta_x = \theta_y = u_0^* = v_0^* = \theta_x^* = \theta_y^* =$ at $y=0, b$
CFCF	$u_0 = v_0 = w_0 = \theta_x = \theta_y = u_0^* = v_0^* = \theta_x^* = \theta_y^* =$ at $x=0, a$

study, the ceramic and the metal material properties are assumed to be temperature-dependent and the details are presented in Table 1. For the computational purpose, different support conditions are employed and detailed in Table 2. The support conditions are not only restricted the rigid body motion but also reduces the total number of unknowns from the desired governing equation.

### 3.1 Convergence and comparison study

The efficacy and the competency of the developed numerical model have been checked initially using the material properties ( $E_m=150$  GPa,  $\nu_m=0.3$  and  $\alpha_m=23.0 \times 10^{-6}$  K $^{-1}$ , for Al and  $E_c=380$  GPa,  $\nu_c=0.3$  and  $\alpha_m=7.4 \times 10^{-6}$  K $^{-1}$  for Al $_2$ O $_3$ , respectively) and support conditions as used by Zhao *et al.* (2009). The convergence behaviour of the buckling load parameters of the square simply-supported FG flat panel ( $a/h=50$ ) is computed for different mesh size and presented in Fig. 2. In this example, the responses of the flat panels are computed for TID material properties. It can be observed that the present results are converging well and a (6 $\times$ 6) mesh is sufficient to compute the further responses.

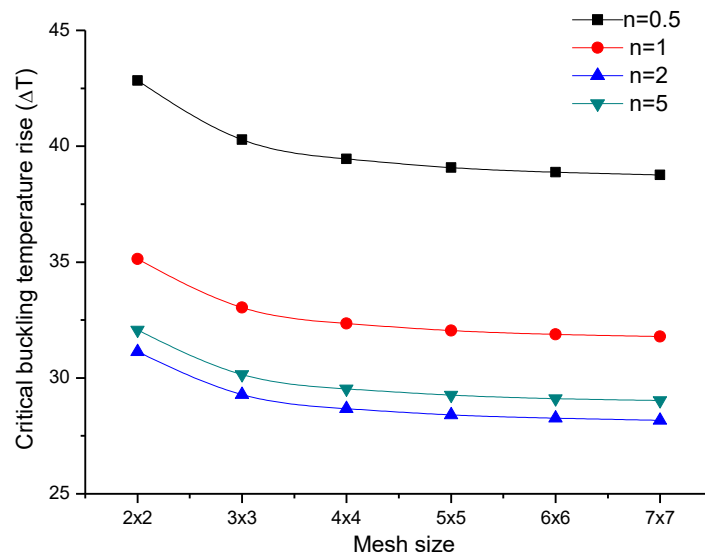


Fig. 2 Convergence behaviour of thermal buckling load parameter of FG (Al/Al $_2$ O $_3$ ) panel ( $a/h=50$ ) for different power-law indices

Now, the present model is extended for the validation purpose to show the efficacy of the proposed FG shell panel model. The critical buckling temperature of the simply-supported FG flat panels is computed for two thickness ratios  $a/h=50$  and  $100$  and presented in Fig. 3. The responses are compared with Zhao *et al.* (2009) and the simulation model developed in ANSYS using APDL code. It is clearly observed that the differences between the reference, ANSYS and present results are very insignificant. It is also interesting to note that the present results are showing higher values as compared to the reference and ANSYS. This is because of the fact that the geometrical stiffness matrix has been modeled based on Green-Lagrange type geometrical nonlinearity including all the nonlinear higher-order terms to capture the geometrical distortion due to the elevated thermal environment which makes the model more flexible as compared to the reference and the simulation cases.

### 3.2 Numerical illustrations

In this section, the effect different material, geometrical and temperature field on the FG shell panel is analysed using the TD and TID properties of silicon nitride ( $Si_3N_4$ ) and stainless steel ( $SUS304$ ) material as in Table 1. The buckling load parameters are computed for four shell geometries by varying the parameters say, power-law indices ( $n$ ), thickness ratios ( $a/h$ ), curvature ratios ( $R/a$ ), aspect ratios ( $a/b$ ) and support conditions. The top and the bottom surface temperatures are assumed to be  $T_c=500^\circ K$  and  $T_m=300^\circ K$ , respectively throughout the analysis if not stated otherwise. The critical thermal buckling load parameter is nondimensionalized as:  $\bar{\lambda}_{cr} = \lambda_{cr} \alpha_0 (T_c - T_m)$ , where  $\alpha_0=1 \times 10^{-6} K^{-1}$ .

#### 3.2.1 Effect of power-law indices

The critical buckling load parameter of simply-supported FG curved shell panel ( $a/b=1$ ,  $a/h=10$ ,  $R/a=5$ ) under the uniform and the linear temperature field with TD and TID properties are computed for four power-law indices ( $n=0.5, 1, 2, 5$ ) and four shell geometries. The responses are presented in Figs. 4(a)-(b) for the uniform and linear temperature field, respectively. It is

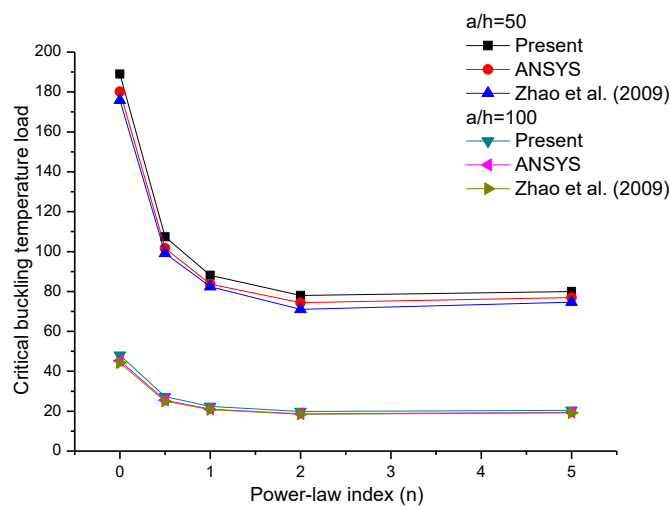


Fig. 3 Comparison study of critical buckling temperature load of FG ( $Al/Al_2O_3$ ) panel ( $a/h=50$  and  $100$ )

clearly observed that the critical load parameters are decreasing as the power-law indices increase irrespective of the panel geometries. It is because as the power-law index increases the FGM turns to metal-rich. It is also true that the ceramic has comparatively higher stiffness than the metal and the responses are within the expected line. The buckling responses are increasing in an ascending order from hyperbolic to spherical i.e., hyperbolic, cylindrical, elliptical, and spherical panel, respectively. The critical buckling load parameters of the FG shell panels are higher for the linear temperature field in comparison to the uniform temperature field irrespective of the geometry and other parameters.

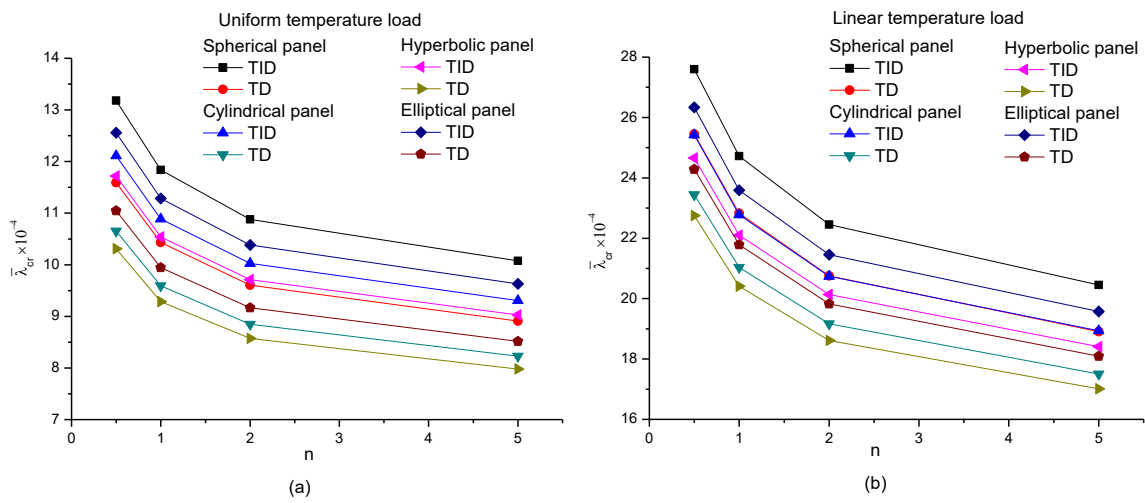


Fig. 4 Nondimensional buckling temperature load parameter of FG curved panels for different power-law indices ( $n=0.5, 1, 2, 5$ ) (a) uniform temperature field (b) linear temperature field

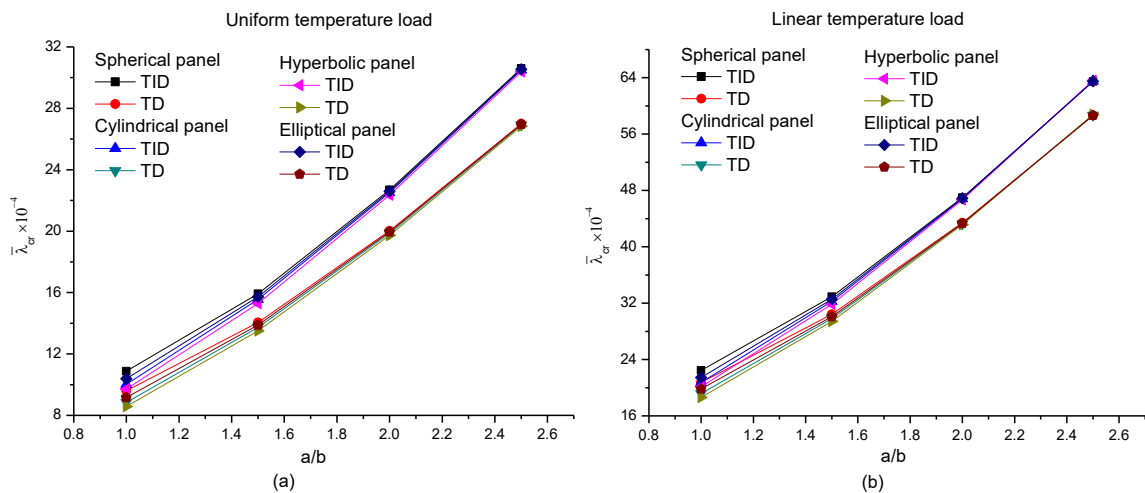


Fig. 5 Effect of aspect ratios ( $a/b=1, 1.5, 2, 2.5$ ) on nondimensional thermal buckling load parameter of FG curved panels (a) uniform temperature field (b) linear temperature field

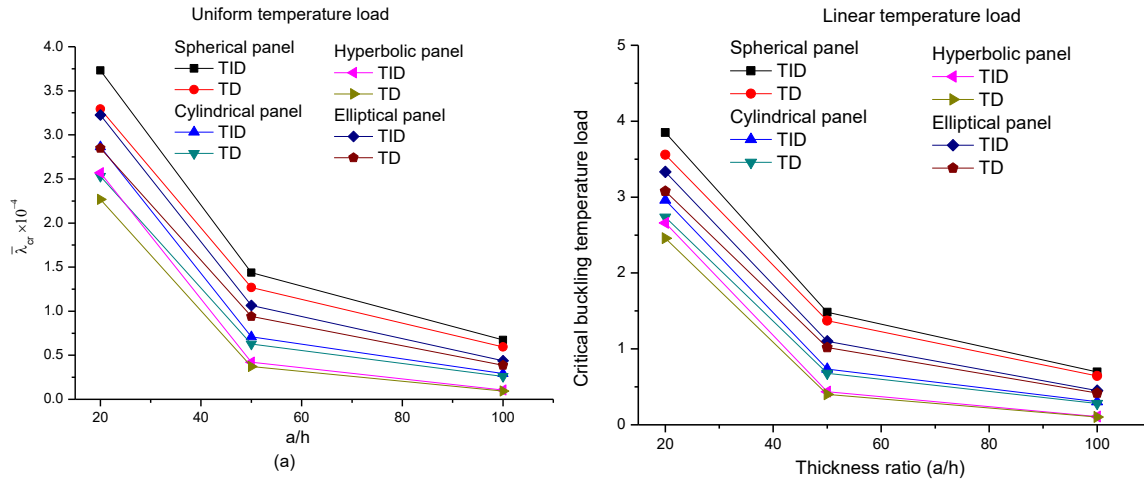


Fig. 6 Effect of thickness ratios ( $a/h=20, 50$  and  $100$ ) on nondimensional buckling load parameter of FG curved panels (a) uniform temperature field (b) linear temperature field

### 3.2.2 Effect of aspect ratio

The effect of aspect ratios ( $a/b=1, 1.5, 2, 2.5$ ) on the critical buckling load parameter of simply-supported FG curved panel ( $a/h=10, n=2, R/a=5$ ) is computed for different temperature field and presented in Figs. 5(a)-(b) for uniform and linear thermal field, respectively. It is noted that the differences in the buckling responses for different FG shell geometries (spherical, cylindrical, hyperbolic and elliptical) are insignificant after  $a/b=2$ .

### 3.2.3 Effect of thickness ratio

Figs. 6(a)-(b) demonstrate the effect of three thickness ratios ( $a/h=20, 50$  and  $100$ ) on the critical buckling temperature load of simply-supported FG curved panels ( $a/b=1, n=2, R/a=5$ ) under the uniform and the linear temperature fields, respectively. The buckling load parameter of the FG curved panel decreases as the thickness ratio increases irrespective of panel geometry. It is also observed that the TD properties of the FG panels have the considerable effect on the buckling responses.

### 3.2.4 Effect of curvature ratio

Table 3 show the effect of curvature ratio ( $R/a=10, 20, 50, 100$ ) on the critical buckling load parameter of simply-supported FG curved panels ( $n=2, a/h=10, a/b=1$ ) under the uniform and the linear temperature field. The buckling load parameter of the FG curved panel reduces with the increment of the curvature ratio except for the hyperbolic panel (may be due to the unequal curvature). The maximum and minimum buckling load parameters are obtained for the spherical and the hyperbolic shell panel, respectively. It is also observed that the buckling load parameters decrease as the curvature ratio increases. It is because as the curvature ratio increases the curved panel approaches to flat one, and the curved panels have higher membrane energy than the flat panels.

### 3.2.5 Effect of support conditions

It is well known that the buckling behaviour of any structure/structural component largely

Table 3 Effect of curvature ratio ( $R/a$ ) on the critical buckling temperature load

Shell geometries	Curvature ratio ( $R/a$ )	Uniform temperature rise		Linear temperature rise	
		TID	TD	TID	TD
Spherical panel ( $R_x=R_y=R$ )	10	5.0175	4.4290	10.3783	9.5917
	20	4.9118	4.3357	10.1708	9.4006
	50	4.8820	4.3094	10.1159	9.3500
	100	4.8777	4.3056	10.1091	9.3439
Cylindrical panel ( $R_x=R$ ; $R_y=\infty$ )	10	4.9105	4.3346	10.1683	9.3983
	20	4.8849	4.3120	10.1208	9.3546
	50	4.8776	4.3055	10.1091	9.3438
	100	4.8765	4.3046	10.1079	9.3428
Hyperbolic panel ( $R_x=R$ ; $R_y=-R$ )	10	4.8712	4.2998	10.0981	9.3338
	20	4.8749	4.3031	10.1057	9.3408
	50	4.8759	4.3040	10.1078	9.3428
	100	4.8761	4.3042	10.1081	9.3430
Elliptical panel ( $R_x=R$ ; $R_y=2R$ )	10	4.9556	4.3743	10.2558	9.4789
	20	4.8962	4.3220	10.1415	9.3735
	50	4.8795	4.3072	10.1118	9.3463
	100	4.8770	4.3050	10.1084	9.3432

Table 4 Effect of support conditions on the critical buckling temperature load of FG curved panels

Shell geometries	Support conditions	Uniform temperature rise		Linear temperature rise	
		TID	TD	TID	TD
Spherical panel ( $R_x=R_y=R$ )	CCCC	12.2467	10.8100	25.3660	23.4330
	SCSC	9.2807	8.1920	19.1953	17.7351
	CFCF	6.2973	5.5585	12.9735	11.9857
Cylindrical panel ( $R_x=R$ ; $R_y=\infty$ )	CCCC	11.8070	10.4220	24.5041	22.6393
	SCSC	8.8062	7.7732	18.2567	16.8700
	CFCF	6.0618	5.3507	12.5250	11.5730
Hyperbolic panel ( $R_x=R$ ; $R_y=-R$ )	CCCC	11.9574	10.5548	24.8663	22.9750
	SCSC	9.0404	7.9801	18.7870	17.3606
	CFCF	6.3112	5.5709	13.0778	12.0843
Elliptical panel ( $R_x=R$ ; $R_y=2R$ )	CCCC	11.9542	10.5518	24.7848	22.8975
	SCSC	8.9554	7.9049	18.5442	17.1348
	CFCF	6.1197	5.4018	12.6261	11.6658

depends on the type of support condition. In this example, the influence of three different support conditions (CCCC, SCSC and CFCF) on the buckling responses of FG single/doubly curved shell panels ( $n=2$ ,  $a/h=10$ ,  $a/b=1$ ,  $R/a=5$ ) are computed for the uniform and the linear temperature fields and presented in Table 4. It is observed that the buckling responses are increasing in the ascending order of CFCF, SCSC, CCCC, i.e., the increase in the number of support restrictions increases the

critical buckling load parameter and the responses are within the expected line. It is also noted that the buckling responses are increasing in an ascending order of the cylindrical, the elliptical, the hyperbolic and the spherical panels.

3.2.5 Buckling mode shapes

Fig. 7(a)-(f) show the buckling mode shapes (first and second) of the FG spherical shell panel ( $a/h=10$ ,  $R/a=5$ ,  $n=2$ ) for three support conditions (SSSS, CCCC and CFCF). The results are computed for the TD material properties under linear temperature field.

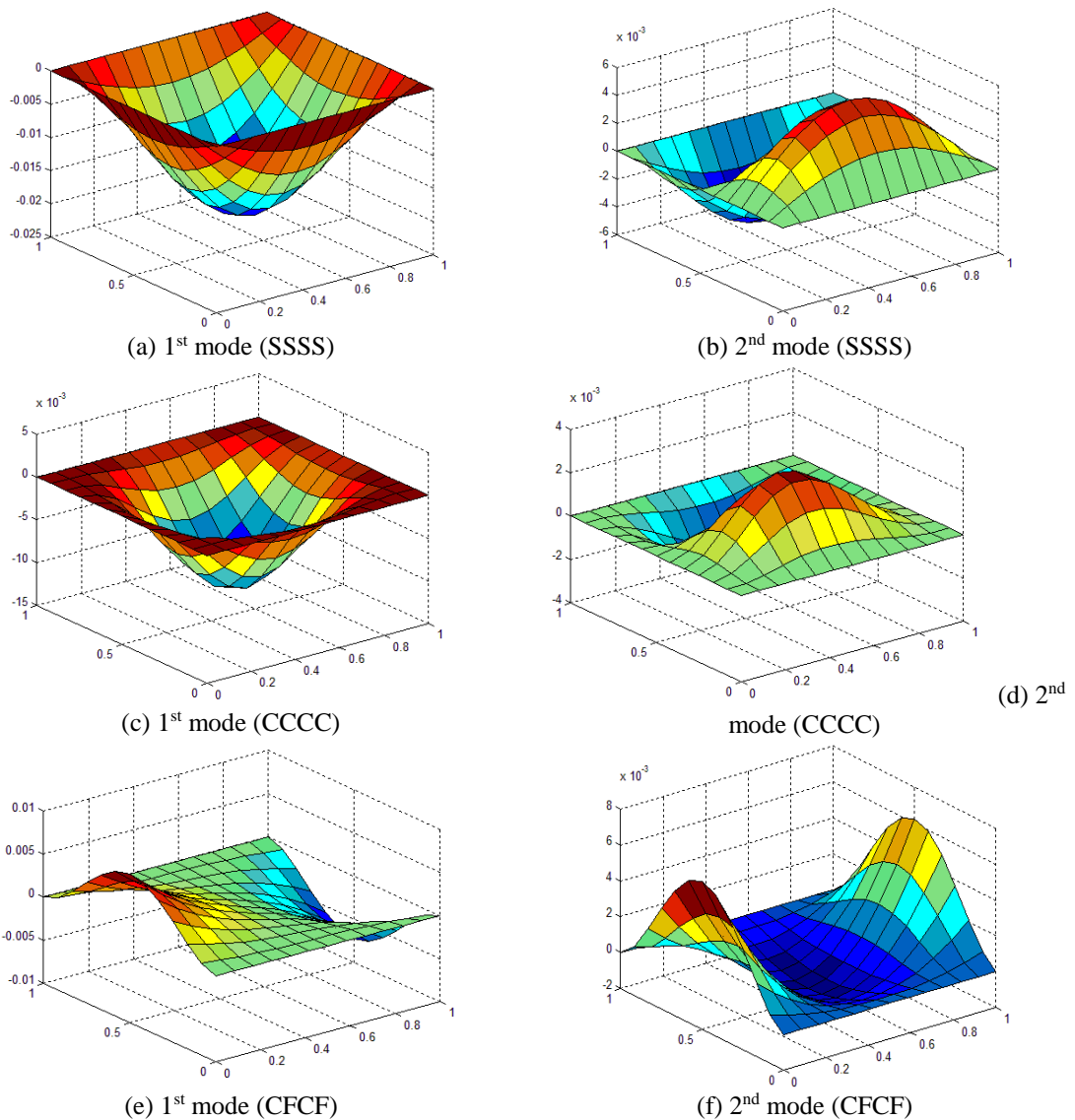


Fig. 7 First and second buckling mode shapes of FG spherical panel under three different support condition (a) 1<sup>st</sup> Mode (SSSS) (b) 2<sup>nd</sup> Mode (SSSS) (c) 1<sup>st</sup> Mode (CCCC) (d) 2<sup>nd</sup> Mode (CCCC) and (e) 1<sup>st</sup> Mode (CFCF) (f) 2<sup>nd</sup> Mode (CFCF)

#### 4. Conclusions

The buckling responses of FG single/doubly curved shell panels (spherical, cylindrical, hyperbolic and elliptical) under the uniform and the linear temperature fields across the thickness direction are examined in this article. The FG shell panel model is developed mathematically using the higher-order kinematic model in conjunction with Green-Lagrange type geometrical nonlinear strain. The material properties of the FGM constituents are considered to be temperature dependent. The effective material properties of the FGM are evaluated using Voigt's micromechanical model via power-law distribution. The governing equation of FG curved panel is derived using variational principle and the desired responses are computed numerically using the FE steps. The efficacy of the present model has been shown by comparing the responses with available published literature and simulation model developed in commercial finite element package (ANSYS) using APDL code. Finally, the comprehensive behaviour of the present model has been shown by computing various numerical examples for different geometrical and material parameters. The following few concluding remarks are made on the numerical experimentation.

- The convergence and comparison study indicate the efficacy of the proposed higher-order model in conjunction with Green-Lagrange nonlinearity for the thermal distortion.
- It is also observed that the temperature dependent material properties have the considerable effect on the buckling behaviour of FG structure under various type of thermal loading.
- The critical buckling load parameters of the FG curved panels are obtained minimum for thin panels, square geometry and fully metal-rich. In addition, it is also seen that the responses are minimum for CFCF support as compared to other support cases.
- It is clear from the analysis that, the critical buckling load parameters are the maximum for spherical shell panels in comparison to all the other geometries are analysed.
- Finally, it is understood that the critical buckling load parameters of the FG curved panels are almost doubled under the linear thermal field in comparison to the uniform field across the thickness direction.

#### References

- Abdelhak, Z., Hadji, L., Daouadji, T.H. and Bedia, E.A. (2015), "Thermal buckling of functionally graded plates using a n-order four variable refined theory", *Adv. Mat. Res.*, **4**(1), 31-44.
- Belabed, Z., Houari, M.S.A., Tounsi, A., Mahmoud, S.R. and Beg, O.A. (2014), "An efficient and simple higher order shear and normal deformation theory for functionally graded material (FGM) plates", *Composites: Part B*, **60**, 274-283.
- Bellifa, H., Benrahou, K.H., Hadji, L., Houari, M.S.A. and Tounsi, A. (2016), "Bending and free vibration analysis of functionally graded plates using a simple shear deformation theory and the concept the neutral surface position", *J. Braz. Soc. Mech. Sci. Eng.*, **38**(1), 265-275.
- Bennoun, M., Houari, M.S.A. and Tounsi, A. (2016), "A novel five variable refined plate theory for vibration analysis of functionally graded sandwich plates", *Mech. Adv. Mater. Struct.*, **23**(4), 423-431.
- Bouderba, B., Houari, M.S.A. and Tounsi, A. (2013), "Thermomechanical bending response of FGM thick plates resting on Winkler-Pasternak elastic foundations", *Steel Compos. Struct.*, **14**(1), 85-104.
- Bouiadjra, M. B., Houari, M. S. A. and Tounsi, A. (2012), "Thermal buckling of functionally graded plates according to a four-variable refined plate theory", *J. Therm. Stress.*, **35**(8), 677-694.
- Bounouara, F., Benrahou, K.H., Belkorissat, I. and Tounsi, A. (2016), "A nonlocal zeroth-order shear deformation theory for free vibration of functionally graded nanoscale plates resting on elastic

- foundation”, *Steel Compos. Struct.*, **20**(2), 227-249.
- Bourada, F., Amara, K. and Tounsi, A. (2016), “Buckling analysis of isotropic and orthotropic plates using a novel four variable refined plate theory”, *Steel Compos. Struct.*, **21**(6), 1287-1306.
- Bourada, M., Kaci, A., Houari, M.S.A. and Tounsi, A. (2015), “A new simple shear and normal deformations theory for functionally graded beams”, *Steel Compos. Struct.*, **18**(2), 409-423.
- Bourada, M., Tounsi, A., Houari, M.S.A., Abbes, E. and Bedia, A. (2011), “A new four-variable refined plate theory for thermal buckling analysis of functionally graded sandwich plates”, *J. Sandwich Struct. Mater.*, **14**(1), 5-33.
- Bousahla, A.A., Houari, M.S.A., Tounsi, A. and Bedia, E.A. (2014), “A novel higher order shear and normal deformation theory based on neutral surface position for bending analysis of advanced composite plates”, *Int. J. Computat. Method*, **11**(6), 1350082.
- Cook, R.D., Malkus, D.S., Plesha, M.E. and Witt, R.J. (2009), *Concepts and Applications of Finite Element Analysis*, John Wiley & Sons, Singapore.
- Daouadji, T.H., Adim, B. and Benferhat, R. (2016), “Bending analysis of an imperfect FGM plates under hygro-thermo-mechanical loading with analytical validation”, *Adv. Mat. Res.*, **5**(1), 35-53.
- Ganapathi, M. and Prakash, T. (2006), “Thermal buckling of simply supported functionally graded skew plates”, *Compos. Struct.*, **74**(2), 247-250.
- Ganapathi, M., Prakash, T. and Sundararajan N. (2006), “Influence of functionally graded material on buckling of skew plates under mechanical loads”, *J. Eng. Mech.*, **132**(8), 902-905.
- Ghannadpour, S.A.M., Ovesy, H.R. and Nassirnia, M. (2012), “Buckling analysis of functionally graded plates under thermal loadings using the finite strip method”, *Comput. Struct.*, **108**, 93-99.
- Gibson, L.J. Ashby, M.F., Karam, G.N., Wegst, U. and Shercliff, H.R. (1995), “Mechanical properties of natural materials. II. Microstructures for mechanical efficiency”, *Proceedings of Royal Society-A*, **450**, 141-162, July.
- Hamidi, A., Houari, M.S.A., Mahmoud, S.R. and Tounsi, A. (2015), “A sinusoidal plate theory with 5-unknowns and stretching effect for thermomechanical bending of functionally graded sandwich plates”, *Steel Compos. Struct.*, **18**(1), 235-253.
- Hebali, H., Tounsi, A., Houari, M., Bessaim, A. and Bedia, E.A. (2014), “A new quasi-3D hyperbolic shear deformation theory for the static and free vibration analysis of functionally graded plates”, *J. Eng. Mech.*, **140**(2), 374-383.
- Houari, M.S.A., Tounsi, A., Bessaim, A. and Mahmoud, S.R. (2016), “A new simple three-unknown sinusoidal shear deformation theory for functionally graded plates”, *Steel Compos. Struct.*, **22**(2), 257-276.
- Javaheri, R. and Eslami, M.R. (2002), “Buckling of functionally graded plates under in-plane compressive loading”, *J. Appl. Math. Mech.*, **82**(4), 277-283.
- Javaheri, R. and Eslami, M.R. (2002), “Thermal buckling of functionally graded plates”, *AIAA J.*, **40**(1), 162-169.
- Javaheri, R. and Eslami, M.R. (2002), “Thermal buckling of functionally graded plates based on higher order theory”, *J. Therm. Stress.*, **25**(7), 603-625.
- Kar, V.R. and Panda, S.K. (2015), “Thermoelastic analysis of functionally graded doubly curved shell panels using nonlinear finite element method”, *Compos. Struct.*, **129**, 202-212.
- Kar, V.R. and Panda, S.K. (2015), “Nonlinear thermomechanical deformation behaviour of P-FGM spherical shallow shell panel”, *Chinese J. Aeronautics*, doi:10.1016/J.CJA.2015.12.007
- Lanhe, W. (2004), “Thermal buckling of a simply supported moderately thick rectangular FGM plate”, *Compos. Struct.*, **64**(2), 211-218.
- Mahapatra, T.R. and Panda, S.K. (2015a), “Nonlinear free vibration analysis of laminated composite spherical shell panel under elevated hygrothermal environment: A micromechanical approach”, *Aero. Sci. Technol.*, doi:10.1016/J.AST.2015.12.018
- Mahapatra, T.R., Panda, S.K. and Kar, V.R. (2015b), “Nonlinear hygro-thermo-elastic vibration analysis of doubly curved composite shell panel using finite element micromechanical model”, *Mech. Adv. Mater. Struct.*, doi:10.1080/15376494.2015.1085606
- Mahi, A., Bedia, E.A.A. and Tounsi, A. (2015), “A new hyperbolic shear deformation theory for bending and

- free vibration analysis of isotropic, functionally graded, sandwich and laminated composite plates”, *Appl. Math. Model.*, **39**(9), 2489-2508.
- Mehar, K., Panda, S.K., Dehengia, A, and Kar V.R. (2015), “Vibration analysis of functionally graded carbon nanotube reinforced composite plate in thermal environment”, *J. Sandwich Struct. Mater.*, doi: 10.1177/1099636215613324.
- Meziane, M.A.A., Abdelaziz, H.H. and Tounsi, A. (2014), “An efficient and simple refined theory for buckling and free vibration of exponentially graded sandwich plates under various boundary conditions” *J. Sandwich Struct. Mater.*, **16**(3), 293-318.
- Na, K.S. and Kim, J.H. (2004), “Three-dimensional thermal buckling analysis of functionally graded materials”, *Compos. Part B-Eng.*, **35**(5), 429-437.
- Panda, S.K. and Singh, B.N. (2009), “Thermal post-buckling behaviour of laminated composite cylindrical/hyperboloidal shallow shell panel using nonlinear finite element method”, *Compos. Struct.*, **91**(3), 366-384.
- Panda, S.K. and Singh, B.N. (2010a), “Nonlinear free vibration analysis of thermally post-buckled composite spherical shell panel”, *Int. J. Mech. Mater. Des.*, **6**(2), 175-188.
- Panda, S.K. and Singh, B.N. (2010b), “Thermal post-buckling analysis of laminated composite spherical shell panel embedded with SMA fibres using nonlinear FEM”, *Proc. IMechE Part C: J. Mech. Eng. Sci.*, **224**(4), 757-769.
- Panda, S.K. and Singh, B.N. (2011), “Large Amplitude Free Vibration Analysis of Thermally Post-buckled Composite Doubly Curved Panel using Nonlinear FEM”, *Finite Element. Anal. Des.*, **47**(4), 378-386.
- Panda, S.K. and Singh, B.N. (2013), “Nonlinear Finite Element Analysis of Thermal Post-buckling Vibration of Laminated Composite Shell Panel Embedded with SMA fibre”, *Aero. Sci. Technol.*, **29**(1), 47-57.
- Panda, S.K. and Singh, B.N. (2013a), “Large amplitude free vibration analysis of thermally post-buckled composite doubly curved panel embedded with SMA fibres”, *Nonlin. Dyn.*, **74**(1-2), 395-418.
- Panda, S.K. and Singh, B.N. (2013b), “Thermal post-buckling analysis of laminated composite shell panel using NFEM”, *Mech. Based. Des. Struct. Mach.*, **41**(4), 468-488.
- Panda, S.K. and Singh, B.N. (2013c), “Postbuckling analysis of laminated composite doubly curved panel embedded with SMA fibres subjected to thermal environment”, *Mech. Adv. Mater. Struct.*, **20**(10), 842-853.
- Pradyumna, S. and Bandyopadhyay, J.N. (2010), “Free vibration and buckling of functionally graded shell panels in thermal environments”, *Int. J. Struct. Stab. Dyn.*, **10**(5), 1031-1053.
- Reddy, J.N. and Chin, C.D. (1998), “Thermomechanical analysis of functionally graded cylinders and plates”, *J. Therm. Stress.*, **21**(6), 593-626.
- Shahsiah, R. and Eslami, M.R. (2003), “Thermal buckling of functionally graded cylindrical shell”, *J. Therm. Stress.*, **26**(3), 277-294.
- Shariat, B.A.S. and Eslami, M.R. (2005), “Effect of initial imperfections on thermal buckling of functionally graded plates”, *J. Therm. Stress.*, **28**(12), 1183-1198.
- Shariat, B.A.S. and Eslami, M.R. (2006), “Thermal buckling of imperfect functionally graded plates”, *Int. J. Solids Struct.*, **43**(14-15), 4082-4096.
- Shariat, B.A.S. and Eslami, M.R. (2007), “Buckling of thick functionally graded plates under mechanical and thermal loads”, *Compos. Struct.*, **78**(3), 433-439.
- Shariat, B.A.S., Javaheri, R. and Eslami, M.R. (2005), “Buckling of imperfect functionally graded plates under in-plane compressive loading”, *Thin-Wall. Struct.*, **43**(7), 1020-1036.
- Shen, H.S. (2009), *Functionally Graded Material: Nonlinear Analysis of Plates and Shells*, CRC press, Boca Raton, FL.
- Thai, H.T. and Choi, D.H. (2012), “An efficient and simple refined theory for buckling analysis of functionally graded plates”, *Appl. Math. Model.*, **36**(3), 1008-1022.
- Topal, U. and Uzman, Ü. (2009), “Thermal buckling load optimization of angle-ply laminated cylindrical shells”, *Int. J. Mater. Des.*, **30**(3), 532-536.
- Tounsi, A., Houari, M.S.A. and Bessaim, A. (2016), “A new 3-unknowns non-polynomial plate theory for buckling and vibration of functionally graded sandwich plate”, *Struct. Eng. Mech.*, **60**(4), 547-565.

- Tounsi, A., Houari, M.S.A., Benyoucef, S. and Adda Bedia, E.A. (2013), "A refined trigonometric shear deformation theory for thermoelastic bending of functionally graded sandwich plates", *Aero. Sci. Tech.*, **24**(1), 209-220.
- Yahia, S.A., Atmane, H.A., Houari, M.S.A. and Tounsi, A. (2015), "Wave propagation in functionally graded plates with porosities using various higher-order shear deformation plate theories", *Struct. Eng. Mech.*, **53**(6), 1143-1165.
- Zhao, X.Y., Lee, Y. and Liew, K.M. (2009), "Mechanical and thermal buckling analysis of functionally graded plates", *Compos. Struct.*, **90**(2), 161-171.
- Zidi, M., Tounsi, A., Houari, M.S.A. and Beg, O.A. (2014), "Bending analysis of FGM plates under hygro-thermo-mechanical loading using a four variable refined plate theory", *Aero. Sci. Tech.*, **34**, 24-34.

CC